

## Highly Isolated 4-Port UWB MIMO Antenna for Next Generation Communication System

Anila Hanif<sup>1</sup>, Shahid Bashir<sup>1</sup>, Anam Hanif<sup>2</sup>

<sup>1</sup>Electrical Engineering University of Engineering and Technology, Peshawar, Pakistan

<sup>2</sup>Electrical Engineering Department, Wah Engineering College, University of Wah, Wah Cantt 47040, Pakistan

\*Correspondence: [anilahhanif@uetpeshawar.edu.pk](mailto:anilahhanif@uetpeshawar.edu.pk), [shahid.bashir@uetpeshawar.edu.pk](mailto:shahid.bashir@uetpeshawar.edu.pk), [anamhanif.ec@gmail.com](mailto:anamhanif.ec@gmail.com)

**Citation** | Hanif. A, Bashir. S, Hanif. A, “Highly Isolated 4-Port UWB MIMO Antenna for Next Generation Communication System”, IJIST, Vol. 07 Special Issue. pp 95-109, May 2025

**Received** | April 09, 2025 **Revised** | May 02, 2025 **Accepted** | May 06, 2025 **Published** | May 08, 2025.

This paper presents the design, optimization, and performance analysis of a compact four-port ultra-wideband (UWB) MIMO antenna for next-generation high-frequency communication systems. The antenna is built on a Rogers RT Duroid 5880 substrate and operates effectively in the 12.5–55 GHz, range making it suitable for millimeter-wave 5G applications. A four-step design process is used to develop a single antenna element optimized for wide bandwidth and good impedance matching. Parametric studies on feedline length, inset depth, and ground structure help improve bandwidth and ensure strong radiation patterns. In the MIMO setup, four radiating elements are placed at right angles to each other to reduce mutual coupling. Additionally, a centrally located plus-shaped decoupling resonator is added to further improve isolation, especially at lower frequencies, enhancing overall antenna performance. Simulation results show excellent impedance matching, a very low envelope correlation coefficient ( $ECC < 0.004$ ), and a high diversity gain (9.98 dB). The antenna also delivers stable radiation patterns and high efficiency (>85 %) across the operating range. These findings confirm that the proposed MIMO antenna offers strong isolation (<-20dB), compact size (20x20 mm<sup>2</sup>), and wide bandwidth (40GHz) making it a suitable choice for future UWB and millimeter-wave MIMO systems.

**Keywords:** UWB Antenna, MIMO Antenna, Mutual Coupling, Millimeter Wave, Wireless Communication.



## Introduction:

The evolution of wireless communication has driven the rapid growth of technologies like 5G, which require high data rates, low latency, and efficient use of the spectrum [1], [2], [3], [4], [5]. UWB and MIMO antennas play a role in meeting these demands by increasing channel capacity and reducing the effects of multipath fading [6], [7]. As millimeter-wave (mm-wave) frequencies become essential for next-generation networks, MIMO antenna designs must overcome challenges such as mutual coupling and impedance matching [8]. Techniques like Defected Ground Structures (DGS) [9], Electromagnetic Bandgap (EBG) structures [10], and parasitic elements [11] have been used to enhance performance. Their Combination [12], [13] and the use of advanced decoupling networks [14] have shown potential in improving isolation and gain in compact MIMO antennas.

Recent developments in MIMO antenna design for 5G and mm-wave applications have achieved high isolation and efficiency. Designs like palm tree-shaped and stepped-shaped antennas have shown isolation levels above 60 dB and 20 dB, respectively, along with wide bandwidth and high radiation efficiency [12], [13]. Tri-band and wideband antennas using passive decoupling have achieved low envelope correlation coefficients (ECCs below 0.007) and over 90% efficiency [14], [15]. A compact 4-port MIMO antenna built on RT/duroid5880 with a defected ground structure demonstrated over 34.2 dB isolation and a gain of 8.72dBi [16]. Other advancements include a compact antenna operating from 26 to 40 GHz, offering an ECC below 0.5 and isolation better than  $-15$  dB, supporting effective diversity performance [17]. An elliptically inspired microstrip antenna designed for V-band 5G applications achieved high gain (8–10.1 dBi), low ECC (0.006), and reduced coupling in a 4-port configuration, enabling high-speed communication [18]. Similarly, a compact 28 GHz MIMO antenna using polarized diversity and fabricated on a Roger RT5880LZ substrate showed excellent performance: 6 dBi gain, 94 % radiation efficiency, 9 GHz bandwidth, and excellent isolation over 24 dB isolation, all without any additional decoupling structures [19]. Another UWB MIMO antenna designed for 25–50 GHz applications used a defected ground structure and orthogonal element layout, resulting in high isolation (better than  $-10$  dB), very low ECC ( $<0.005$ ), and strong diversity gain (about 10 dB) [20].

A separate study targeting MIMO performance improvement at 30 GHz employed Curved Edges (CE), DGS, and Band Gap Structures (BGS) to enhance isolation from  $-21.4$  dB to  $-27.2$ . It also achieved a 7.5 dBi gain and maintained S11 at  $-35$  dB [21]. Although these techniques reduce surface current and improve isolation. Integrating UWB with MIMO remains challenging due to tradeoff between high isolation and compact cost-effective design.

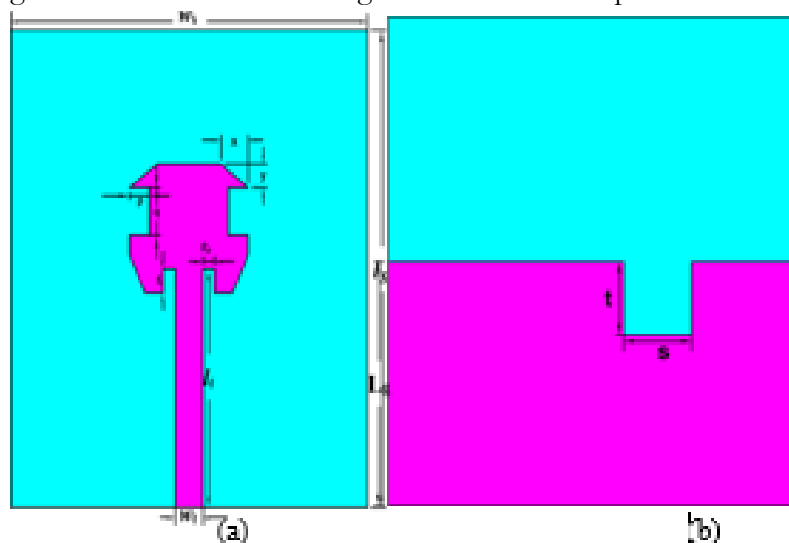


**Figure 1.** Single element design (a) Top view (b) Bottom view

This paper aims to develop a compact four-port UWB- MIMO antenna with improved isolation and wideband features. The design introduces a novel decoupling structure to minimize mutual coupling, thereby enhancing isolation, efficiency, and gain without increasing the antenna's size. The goal is to strike the right balance between compact design and high performance, contributing to advanced antenna solutions for future communication systems.

The structure of the paper is as follows: Section II, describes the design and methodology of the proposed 4-port UWB MIMO antenna, including isolation and optimization strategies. Section III presents simulation results and performance metrics, while Section IV concludes the study.

### Methodology:

The design methodology followed in this work is illustrated in Figure 4. It starts with the initial patch design, followed by parametric optimization. If the desired bandwidth and impedance matching are achieved, the next step is array configuration. If not, the parameters are re-optimized until the goals are met.

### Single Element Design:

For ultra-wideband (UWB) applications, an antenna is designed using Rogers RT Duroid 5880 due to its high-frequency support and low-loss characteristics. The  $10 \times 9 \text{ mm}^2$  single antenna element, shown in Figure 1 was developed through a four-step design process to achieve the desired resonance frequency while ensuring UWB performance for advanced wireless communication systems. The antenna design process illustrated in Figures 2(a-d), with the reflection coefficient results shown in Figure 3 and the current distribution in Figure 5(a-d). The initial square microstrip patch antenna (Figure 2a) shows poor impedance matching and weak radiation, as observed in Figure 3 and Figure 5a. To improve performance, the ground plane is truncated and the patch corners are etched (Figure 2b), which enhances impedance matching and radiation efficiency, as confirmed by Figure 3 and Figure 5b. Next, a rectangular slot is introduced in the patch (Figure 2c) reduces), reducing reflection loss and improving surface current distribution (Figure 5c).

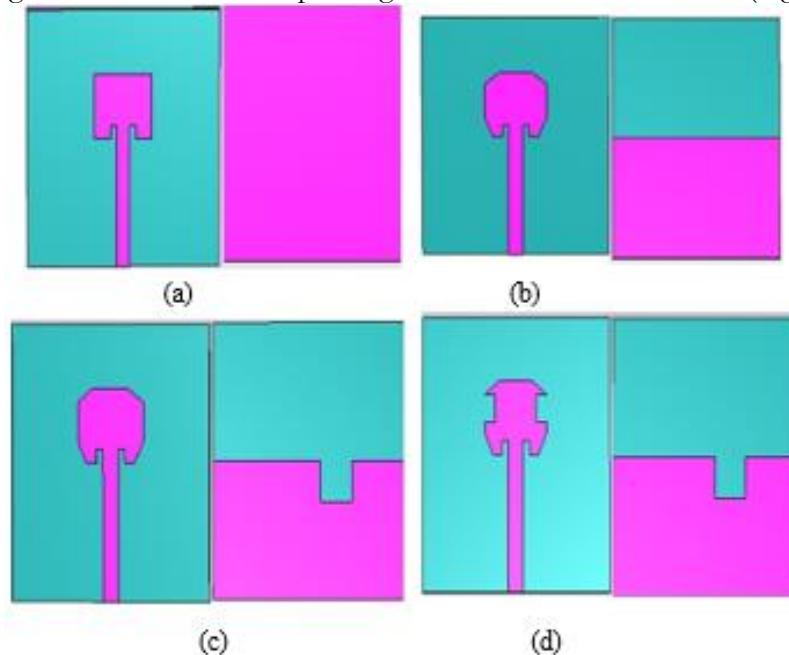


**Figure 2.** Design steps (a) 1<sup>st</sup> step (b) 2<sup>nd</sup> step (c) 3<sup>rd</sup> step (d) 4<sup>th</sup>

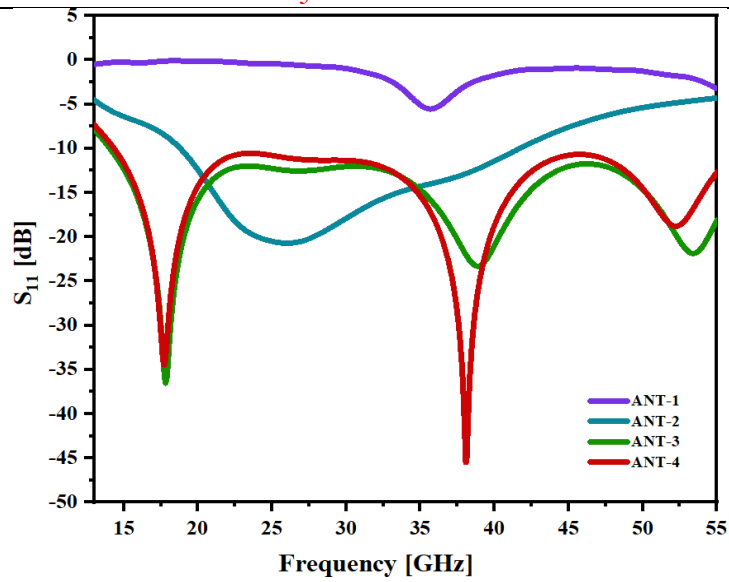


Figure 3.  $S_{11}$  of the different design steps

Table 1. Parametric table.

Parameter	Value (mm)
$l_s$	10
$W_s$	9
$l_f$	5
$w_f$	0.7
$x$	0.7
$y$	0.5
$p$	0.5
$q$	1
$L_g$	5
$s$	1.5
$t$	1.5
$g_p$	0.3
$f_i$	0.5

Finally, adding side slots (Figure 2d) extends the UWB response and ensures efficient radiation, validated by the results in Figure 3 and Figure 5d. Design specifications for the antenna are summarized in Table 1. The resonant frequency and impedance characteristics of a patch antenna mainly depend on its length and width. The patch width  $w_p$  is calculated using

$$w_p = \frac{c}{2f_o \sqrt{\frac{\epsilon_r + 1}{2}}} \quad (1)$$

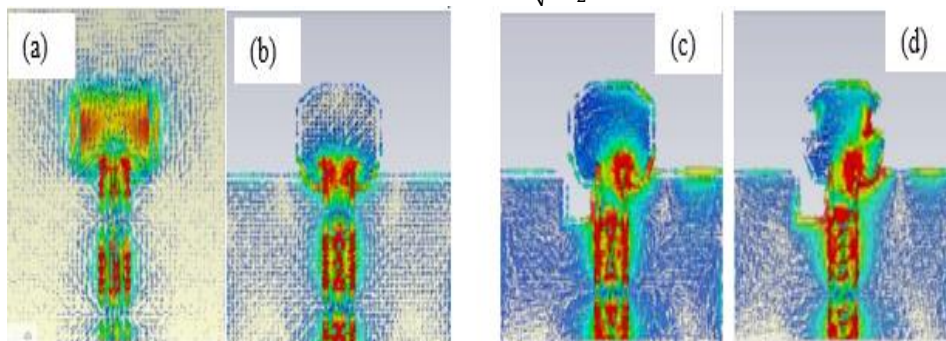


Figure 4. Current distribution (a) step 1 (b) step 2 (c) step 3 (d) step 4

where  $c$  is the speed of light,  $f_0$  is the resonant frequency, and  $\epsilon_r$  is the substrate's relative permittivity. The effective dielectric constant  $\epsilon_{eff}$  is given by

$$\epsilon_{eff} = \frac{\epsilon_r + 1}{2} + \frac{\epsilon_r - 1}{2} \left[ 1 + 12 \frac{h}{w_p} \right]^{-1} \quad (2)$$

where  $h$  is the substrate thickness. The actual patch length, considering fringing effects, is  $L_{eff} = \frac{c}{2f_0 \sqrt{\epsilon_{eff}}} \quad (3)$  with the length correction.

**Parametric Analysis:**

The study examines the impact of inset depth ( $f_i$ ), gap ( $g_p$ ), feed line length ( $l_f$ ), and ground length ( $L_g$ ) on the performance of a UWB MIMO antenna. The results show optimal impedance matching and a wideband response (15-55 GHz) with  $f_i=0.5$  and  $l_f=5$  (Figure(6a-d)). The study emphasizes the importance of fine-tuning these parameters to achieve the desired operating characteristics.

**Configuration of UWB MIMO Antenna:**

The proposed ultra-wideband (UWB) MIMO antenna, as shown in Figure 7, is designed using a Rogers RT Duroid 5880 substrate with a relative permittivity of  $\epsilon_r=2.2$ , a loss tangent of  $\delta=0.0009$ , and a thickness of 0.254 mm. The antenna consists of four radiating elements arranged in an orthogonal pattern to enhance port isolation without the need for additional decoupling techniques. The spacing between adjacent patches is 10.3 mm, and the antenna has a compact size of  $20 \times 20 \times 0.254 \text{ mm}^3$ . All simulations were performed using CST Microwave Studio Suite.

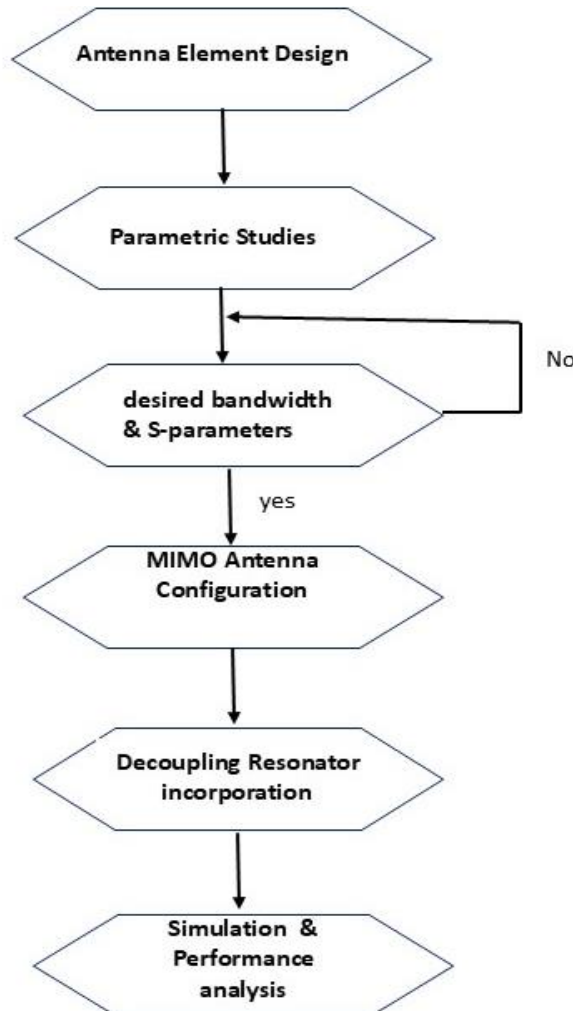
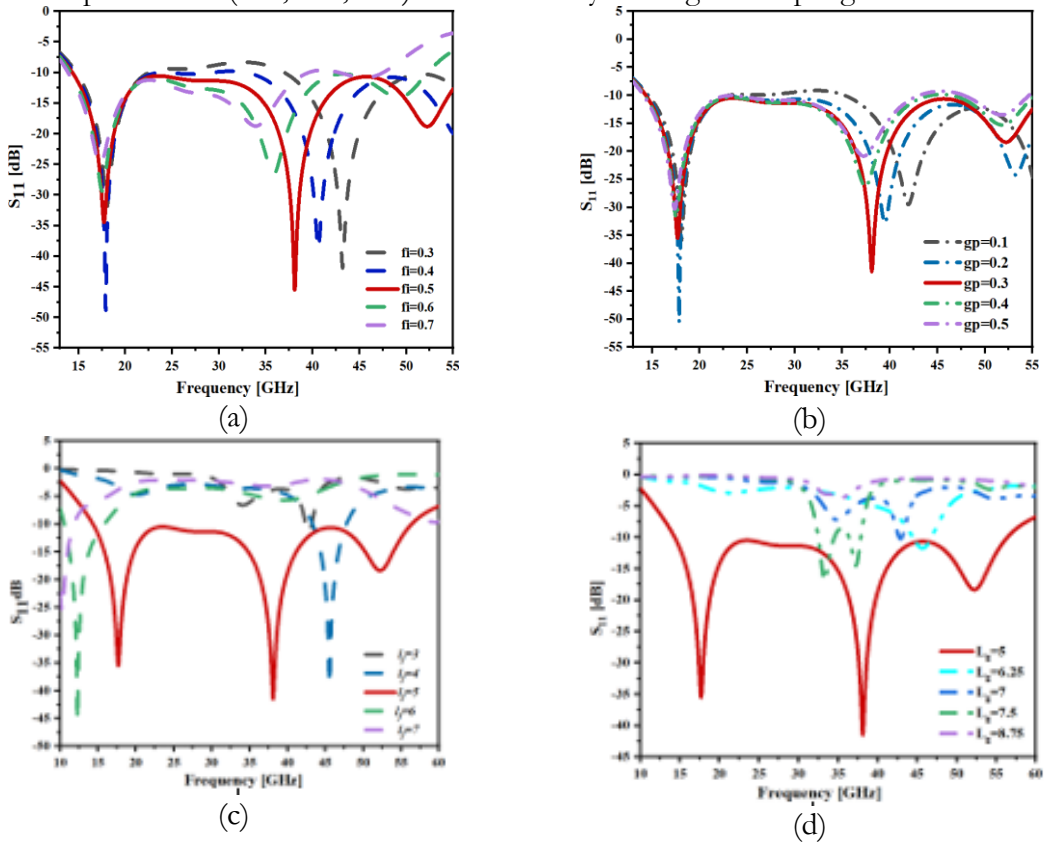


Figure 5. Flow diagram of design methodology

**S-Parameters Response and Mutual Coupling of MIMO:**

The S-parameter response of the proposed 4-port MIMO antenna is shown in Figure 8a. The return loss parameters ( $S_{11}$ ,  $S_{22}$ ,  $S_{33}$ ,  $S_{44}$ ) remain well below  $-10$  dB across the operational bandwidth, indicating effective impedance matching at all ports. Multiple resonance points confirm the antenna's wideband behavior, while consistent resonance across ports reflects stable impedance and uniform excitation.

These characteristics ensure that the multi-port design maintains optimal performance. The performance of the single-element antenna for mm-wave UWB applications is analyzed. The mutual coupling analysis, shown in Figure 8b, reveals increased coupling around 19–20 GHz due to the absence of a decoupling structure. The isolation parameters ( $S_{12}$ ,  $S_{13}$ ,  $S_{14}$ ) are affected by this higher coupling.



**Figure 6.** Optimization of various parameters (a) changing  $f_i$  (b) changing  $g_p$ , (c) changing  $l_i$  (d) changing  $L_g$

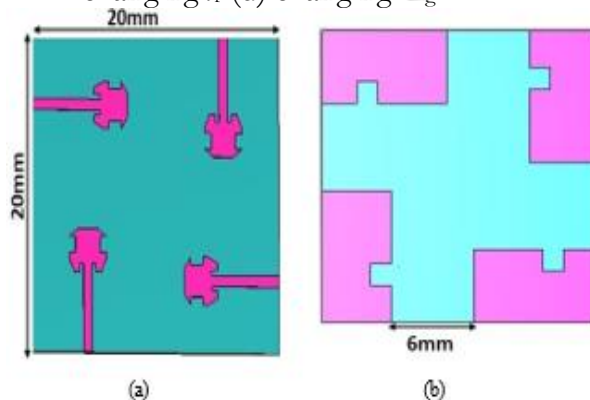


**Figure 7.** Orthogonal arrangement (a). Front View (b). Back View

**Proposed Decoupling Technique:**

Decoupling resonators are essential for reducing mutual coupling in MIMO

antennas, improving isolation, and maintaining signal integrity by resonating at the system's frequency [22]. A plus-shaped decoupling resonator, centrally placed in the MIMO system (Figure 9a), acts as a selective filter to suppress undesired coupling, thereby improving the bandwidth at lower spectrum starting from 12.5–55 GHz while in without decoupling it started from 15–55 GHz. The initial mutual coupling between the antenna elements was relatively high as depicted in (Figure 8b), with  $S_{12}$ ,  $S_{13}$  and  $S_{14}$  around -15 dB. After introducing the decoupling element, as illustrated in Figure 9(b), a significant improvement in isolation is observed. The values of  $S_{12}$ ,  $S_{13}$  and  $S_{14}$  are now consistently below -20 dB across the entire band, with some frequencies reaching isolation levels as low as -60 dB. This clearly demonstrates the effectiveness of the decoupling structure in reducing mutual coupling and enhancing antenna performance.

A parametric study, varying the resonator length (denoted as the  $v$  parameter) from 3.6 mm to 7.6 mm, showed that a length of 5.6 mm resulted in an improved reflection coefficient of approximately -50 dB, as shown in Figure 9c.

**Efficiency and Gain:**

The MIMO antenna’s gain and overall efficiency, shown in Figure 12, provide a comprehensive overview of its performance. The antenna exhibits strong directional radiation characteristics with a peak gain of 6.95 dBi. Additionally, minimal power loss is observed, as the overall efficiency remains above 85% across the entire operating bandwidth.

**MIMO Antenna Performance:**

MIMO technology requires integrating multiple antennas into limited PCB space, with a focus on performance metrics such as Envelope Correlation Coefficient (ECC), Diversity Gain (DG), and Total Active Reflection Coefficient (TARC), along with standard parameters such as bandwidth, radiation efficiency, and gain for performance evaluation [23], [24].

**Envelope Correlation Coefficient (ECC):** The Envelope Correlation Coefficient (ECC) measures signal independence for effective diversity and is typically calculated using radiation patterns or S-parameters [25], [26]. The S-parameter- based ECC is given by Equation (1), where  $\eta_1$  and  $\eta_2$  represent the antenna efficiencies:

$$ECC = \frac{|S_{11}S_{12}^* + S_{21}S_{22}^*|^2}{(1 - |S_{11}|^2 - |S_{21}|^2)(1 - |S_{22}|^2 - |S_{12}|^2)\eta_1\eta_2} \quad (4)$$

The proposed MIMO antenna achieved ECC less than 0.004 with the addition of a plus- shaped decoupling resonator, significantly improving isolation and diversity (Figure 13).

**Diversity Gain (DG):** Diversity Gain (DG) enhances signal reliability in MIMO systems by improving the Signal-to-Noise Ratio (SNR) and is estimated using ECC or CDF methods [27]. It is calculated using:

$$DG = 10 (\sqrt{1 - ECC^2}) \quad (5)$$

As shown in Figure 14, the proposed antenna achieves near- ideal DG (10 dB) after the addition of the decoupling element, ensuring robust diversity performance.

**Total Active Reflection Coefficient (TARC):** In particular, for a four-port network, TARC is defined by [28];

$$TARC = \frac{1}{2} \sqrt{\left\{ \begin{array}{l} |S_{11} + S_{12}e^{j\theta}|^2 + |S_{21} + S_{22}e^{j\theta}|^2 \\ + \\ |S_{31} + S_{32}e^{j\theta}|^2 + |S_{41} + S_{42}e^{j\theta}|^2 \end{array} \right\}} \quad (6)$$

**Simulation and Results:**

**Surface Current Density:**

The surface current distribution is analyzed to evaluate the isolation characteristics

of the proposed MIMO antenna design at two frequencies: 20 GHz and 36 GHz, as shown in Figure 10. At 20 GHz, the distribution without any decoupling element reveals strong coupling between the antenna elements.

However, when decoupling resonators, are introduced, the plus-shaped resonator significantly reduces mutual coupling. Similarly, at 36 GHz, the surface current distributions with and without decoupling elements, shown in Figure 10(c,d), further confirm the superior performance of the plus-shaped resonator.

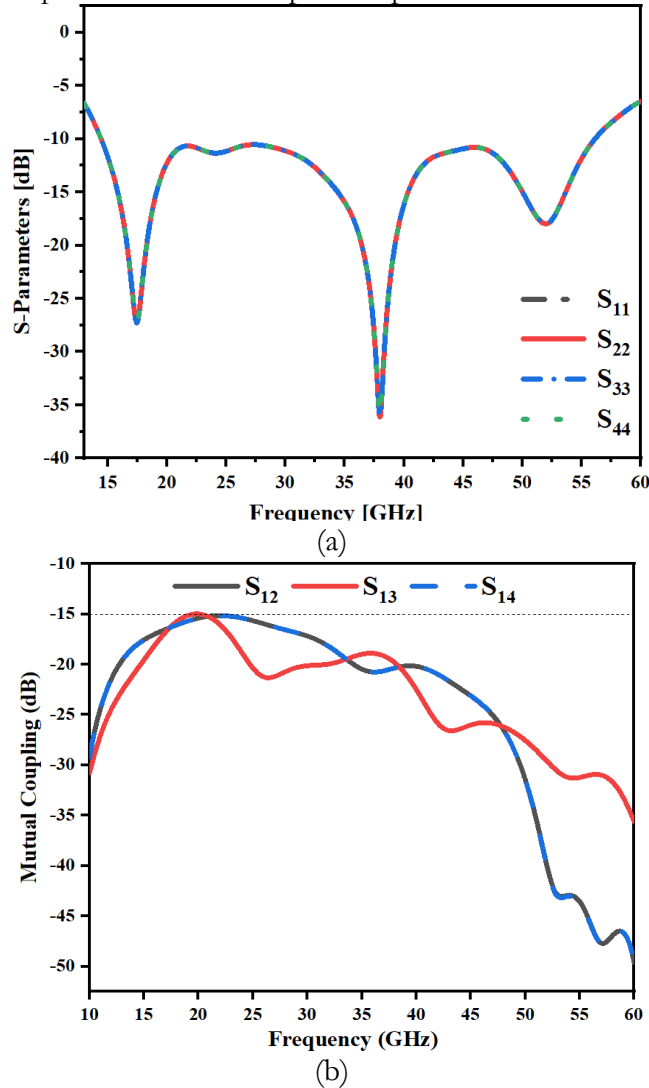


**Figure 8.** (a) Reflection coefficients of MIMO with orthogonal arrangement (b) Mutual coupling without decoupling

**Far Field Measurement:**

The radiation patterns of the proposed MIMO antenna were analyzed at 25 GHz, 36 GHz, and 40 GHz to assess its performance across the operational bandwidth. At 25 GHz, the pattern (Figure 11a) shows a broad lobe, indicating stable radiation characteristics at lower frequencies. At 36 GHz (Figure 11b), the radiation pattern becomes more defined, displaying improved directivity. At 40 GHz (Figure 11c), the pattern evolves with distinct lobes and high directivity, confirming the antenna’s enhanced performance at higher frequencies.

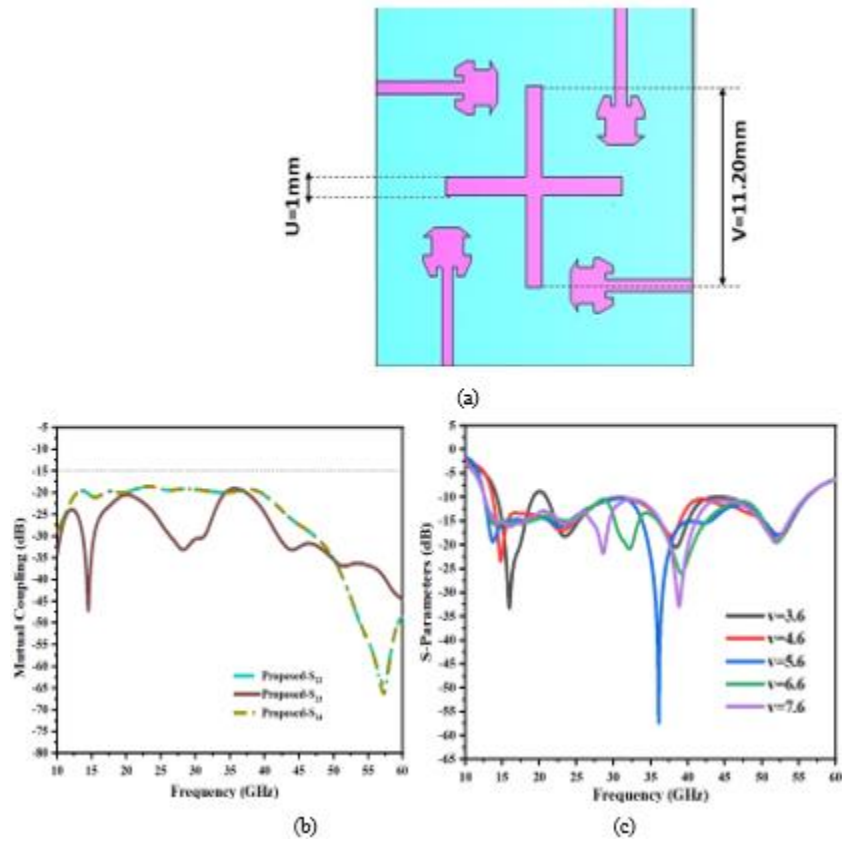


**Figure 9.** (a) UBW MIMO with plus shaped resonator (b) Effect of plus shaped resonator on mutual coupling (c) Effect of variation in v parameter

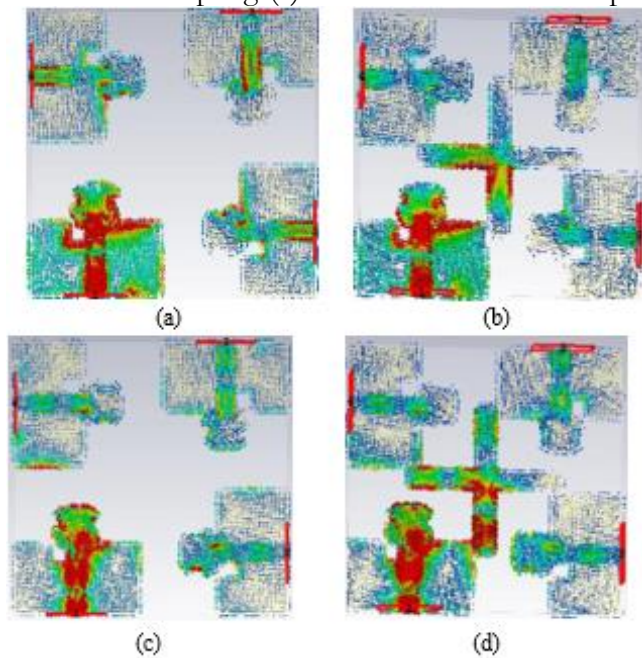


**Figure 10.** Current Distribution at 20 GHz (a) without decoupling (b) with Plus-shape resonator (c) without decoupling at 36GHz (d) with plus-shape resonator at 36 GHZ.

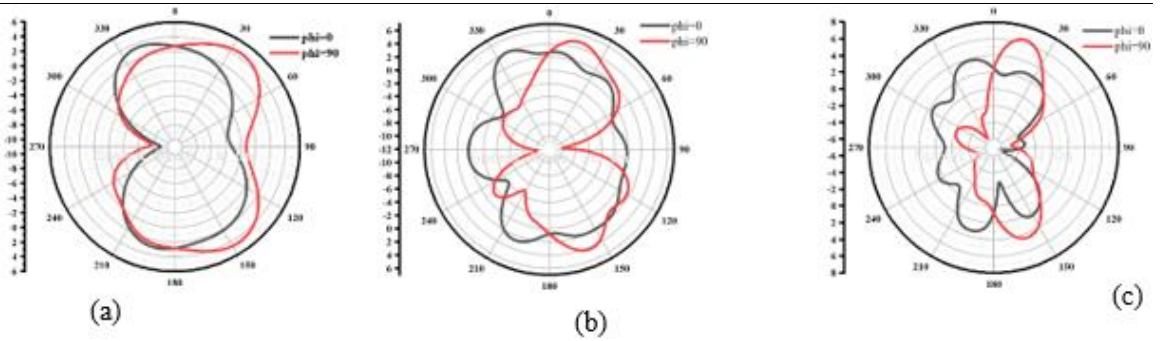


Figure 11. Radiation Pattern (a) 25GHz (b) 36GHz (c) 40GHz

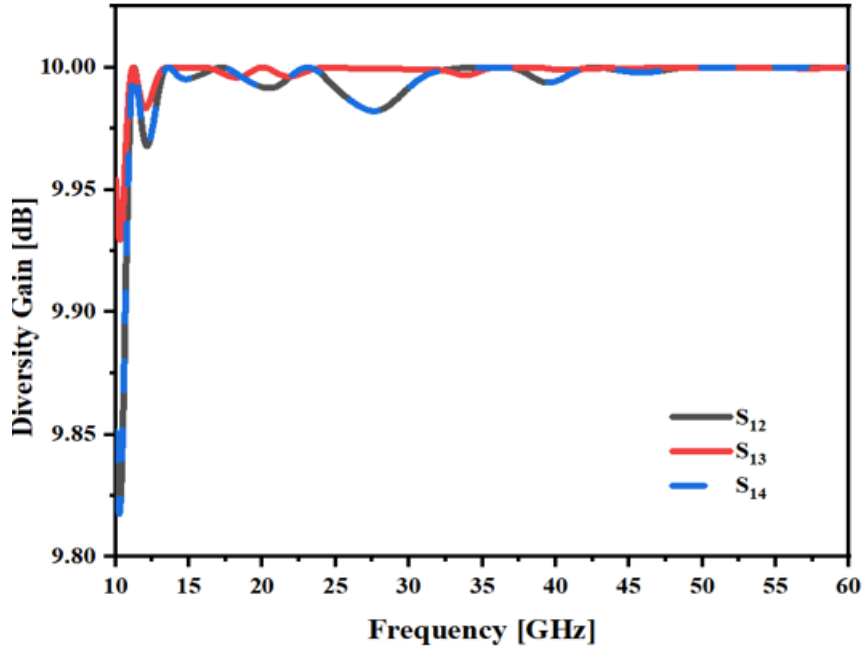


Figure 14. DG of proposed design

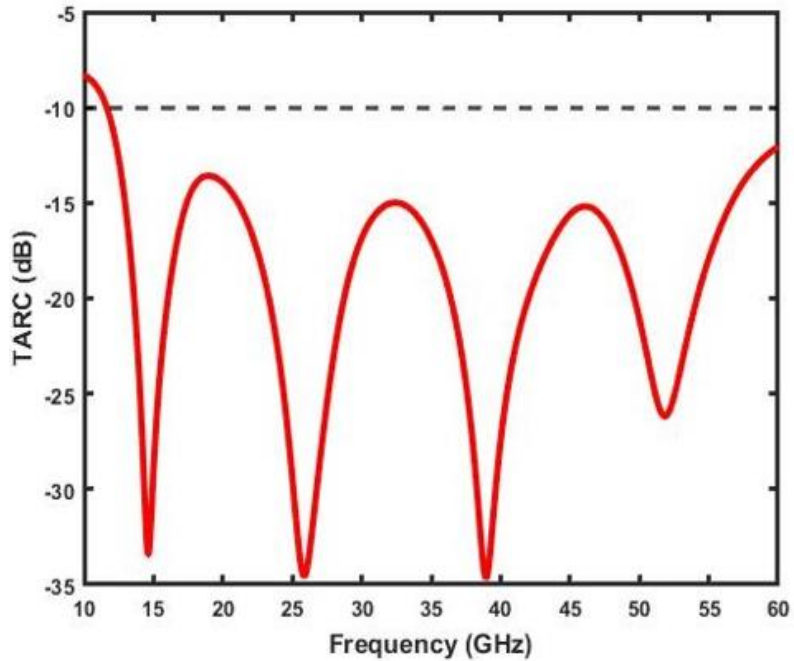


Fig 15. TARC of proposed design

The proposed design shows TARC values below -10 dB across the operational

bandwidth (Figure 15), indicating minimal reflection and efficient power utilization.

**Discussion:**

The performance comparison of the proposed MIMO antenna with recent state-of-the-art designs is summarized in *Table II*. The proposed MIMO antenna addresses the challenges of large size, low bandwidth, and complex design seen in previous state-of-the-art solutions. Different substrate materials with different size, techniques have been applied to achieve desired results. However, the mentioned designs have some drawbacks of either complex structure, large dimensions, complex isolation techniques, low bandwidth which devalue its real-time applications. Hence, our proposed design has a very small dimensions of 20x20mm<sup>2</sup>, with a very large bandwidth of more than 40 GHz and very simple design structure and isolation techniques of plus shaped, which can be considered a very good and proficient candidate for 5G mm-waves application.

**Table 2.** Comparison of Proposed Antenna with Existing Designs

Ref. No.	Size (mm <sup>3</sup> ) [Ports]	Frequency Range (GHz)	Bandwidth (GHz)	Peak Gain (dBi)	Efficiency (%)	Isolation (dB)	ECC	DG	Applied Design Method
[12]	45×50×0.8 [4]	23.4–35	11.6	12.4	—	< -60	<0.0014	9.8	Orthogonal Orientation
[13]	20.48×20.48 ×1.6 [4]	25.21–32.34	7.13	6.87	94	< -20	0.006	9.97	Defected Ground & Isolating Metallic Sheet
[14]	30×30×0.25 [4]	5.2–5.7, 11.8–17.3, 23.4–37.3	0.5, 5.5, 13.9	3.05, 5.27, 6.67	93–98	< -20	<0.004, <0.002, <0.002	>9.9	DGS
[15]	36×18×1.6 [2]	3–40	37	6.3	—	< -20	<0.0005	>9.999	Defected Slotted Ground with Slotted Patch
[16]	25×25×0.787 [4]	25.28–28.02	2.74	8.72	—	23.2	<0.0015	>9.999	DGS
[17]	23×18×0.25 [4]	26–40	14	6.6	>90	< -18	0.001	>9.95	Orthogonal Placement
[18]	26×26×0.25 [4]	52.9–70	17.7	8–10.1	90	< -20	<0.006	>9.98	DGS
[19]	16×16×0.25 [4]	22.2–31.4	9.2	5.98	94	-20	0.00001	9.99	Elliptical Slots & Orientation
Proposed	20×20×0.254 [4]	15–55	40	6.63	>85	< -20	<0.0008	>9.98	DGS, Orthogonal & Plus-Shape Resonator

**Conclusion:**

This paper presented the design and analysis of a 4-port UWB MIMO antenna optimized for next-generation wireless communication. Operating across 12.5–55 GHz, the antenna is well-suited for 5G millimeter-wave and high-speed data applications. A plus-shaped decoupling resonator effectively reduces mutual coupling, improving isolation, particularly in the 19–20 GHz range. Simulation results demonstrate excellent performance, with ECC < 0.004, DG > 9.98, isolation > 15 dB, and TARC < -10 dB. The proposed antenna ensures wideband operation enhanced isolation, and efficient impedance matching, making it a promising solution for advanced wireless systems.

This work can be further extended by experimental fabrication, such as prototype realization and experimental verification in real-world scenarios. In future, fabrication and measurement can be done to validate the results. Flexible substrates can be used to make it suitable for IoT and wearable devices. Isolation can be further improved by using hybrid decoupling methods. Also, the number of antenna elements can be increased to design an 8-port system for higher data rates, but its effect on isolation and bandwidth needs to be studied.

**Acknowledgment:**

The authors declare that they have contributed equally to the conception, execution, and writing of this work. No financial support or benefits from any third party were received in connection with this research.

**References:**

- [1] A. U. R. Chilakala Sudhamani, Mardeni Roslee, Jun Jiat Tiang, “A Survey on 5G Coverage Improvement Techniques: Issues and Future Challenges,” *Sensors*, vol. 23, no. 4, p. 2356, 2023, doi: <https://doi.org/10.3390/s23042356>.
- [2] A. A. O. Yusuf Olayinka Imam-Fulani, Nasir Faruk, Olugbenga A. Sowande, Abubakar Abdulkarim, Emmanuel Alozie, Aliyu D. Usman, Kayode S. Adewole, “5G Frequency Standardization, Technologies, Channel Models, and Network Deployment: Advances, Challenges, and Future Directions,” *Sustainability*, vol. 15, no. 6, p. 5173, 2023, doi: <https://doi.org/10.3390/su15065173>.
- [3] M. K. Hossain, M. M. Rana, and M. R. Haider, “Spectrum-Efficient Analog Pulse Index Modulation for High-Volume Wireless Data Telemetry,” *IEEE Internet Things J.*, vol. 10, no. 11, pp. 9556–9564, Jun. 2023, doi: 10.1109/JIOT.2023.3234262.
- [4] Mina Malekzadeh, “Performance prediction and enhancement of 5G networks based on linear regression machine learning,” *EURASIP J. Wirel. Commun. Netw. Vol.*, 2023, doi: <https://doi.org/10.1186/s13638-023-02282-z>.
- [5] N. G. & A. N. Arun Kumar, “Improving the latency for 5G/B5G based smart healthcare connectivity in rural area,” *Sci. Rep.*, vol. 14, no. 6976, 2024, doi: <https://doi.org/10.1038/s41598-024-57641-7>.
- [6] M. S. E. Anwer S. Abd El-Hameed, Mohamed G. Wahab, Nashwa A. Elshafey, “Quad-Port UWB MIMO antenna based on LPF with vast rejection band,” *AEU - Int. J. Electron. Commun.*, vol. 134, p. 153712, 2021, doi: <https://doi.org/10.1016/j.aeue.2021.153712>.
- [7] S. R. and S. G. X. Zhao, “A Reconfigurable MIMO/UWB MIMO Antenna for Cognitive Radio Applications,” *IEEE Access*, vol. 7, pp. 46739–46747, 2019, doi: 10.1109/ACCESS.2019.2909810.
- [8] Ratan Sanjay D and Syed Azeemuddin, “A comprehensive review of high voltage wideband and ultra-wide band antennas for IEMI applications,” *Eng. Res. Express*, vol. 3, no. 1, 2021, doi: 10.1088/2631-8695/abd873.
- [9] A. K. Ashok Kumar, Ashok Kumar, “Defected Ground Structure Based High Gain, Wideband and High Diversity Performance Quad-Element MIMO Antenna Array for

- 5G Millimeter-Wave Communication,” *Prog. Electromagn. Res.*, vol. 101, pp. 1–16, 2023, doi: 10.2528/PIERB23030601.
- [10] L. Zheng and D. N. C. Tse, “Diversity and multiplexing: A fundamental tradeoff in multiple-antenna channels,” *IEEE Trans. Inf. Theory*, vol. 49, no. 5, pp. 1073–1096, May 2003, doi: 10.1109/TIT.2003.810646.
- [11] G. Casu, L. Tută, I. Nicolaescu, and C. Moraru, “Some aspects about the advantages of using MIMO systems,” *2014 22nd Telecommun. Forum, TELFOR 2014 - Proc. Pap.*, pp. 320–323, 2014, doi: 10.1109/TELFOR.2014.7034415.
- [12] B. T. P. M. Fatima Kiouach, Bilal Aghoutane, Sudipta Das, Mohammed EL Ghzaoui, Tanvir Islam, “A high isolation wideband palm tree-shaped printed  $4 \times 4$  MIMO antenna for 5G mm-waves applications,” *AEU - Int. J. Electron. Commun.*, vol. 179, p. 155322, 2024, doi: <https://doi.org/10.1016/j.aeue.2024.155322>.
- [13] V. G. Poonam Tiwari, Meenu Kaushik, Anshuman Shastri, Pinku Ranjan, “A 28 GHz wideband planar stepped-shaped MIMO antenna with isolating metallic sheet for 5G millimeter wave communications,” *AEU - Int. J. Electron. Commun.*, vol. 184, p. 155411, 2024, doi: <https://doi.org/10.1016/j.aeue.2024.155411>.
- [14] F. A. B. Ayyaz Ali, Mehr E Munir, Moustafa M. Nasralla, Maged A. Esmail, Ahmed Jamal Abdullah Al-Gburi, “Design process of a compact Tri-Band MIMO antenna with wideband characteristics for sub-6 GHz, Ku-band, and Millimeter-Wave applications,” *Ain Shams Eng. J.*, vol. 15, no. 3, p. 102579, 2024, doi: <https://doi.org/10.1016/j.asej.2023.102579>.
- [15] K. V. Prasad, N. Venkateswari, M. Sandhyarani, P. V. Kumar, and K. M. Lakshmi, “Isolation and Bandwidth Enhancement of Compact Wideband MIMO for Sub-6 GHz, Ku-band and Millimeter-Wave with UWB Applications,” *Prog. Electromagn. Res. C*, vol. 148, pp. 83–95, 2024, doi: 10.2528/PIERC24070401.
- [16] S. E. B. K. Cem Güler, “A Novel High Isolation 4-Port Compact MIMO Antenna with DGS for 5G Applications,” *Micromachines*, vol. 14, no. 7, p. 1309, 2023, doi: <https://doi.org/10.3390/mi14071309>.
- [17] M. E. Munir, M. M. Nasralla, and M. A. Esmail, “Four port tri-circular ring MIMO antenna with wide-band characteristics for future 5G and mmWave applications,” *Heliyon*, vol. 10, no. 8, p. e28714, Apr. 2024, doi: 10.1016/J.HELİYON.2024.E28714.
- [18] A. A. I. Wael A.E. Ali, Mahmoud A. Abdelghany, “Wideband and high gain elliptically-inspired  $4 \times 4$  MIMO antenna for millimeter wave applications,” *Heliyon*, vol. 10, no. 20, p. e38697, 2024, [Online]. Available: [https://www.cell.com/heliyon/fulltext/S2405-8440\(24\)14728-7?\\_returnURL=https%3A%2F%2Flinkinghub.elsevier.com%2Fretrieve%2Fpii%2FS2405844024147287%3Fshowall%3Dtrue](https://www.cell.com/heliyon/fulltext/S2405-8440(24)14728-7?_returnURL=https%3A%2F%2Flinkinghub.elsevier.com%2Fretrieve%2Fpii%2FS2405844024147287%3Fshowall%3Dtrue)
- [19] N. Farooq, K. Muzaffar, and S. A. Malik, “Compact Elliptical Slot Millimeter-Wave MIMO Antenna for 5G Applications,” *J. Infrared, Millimeter, Terahertz Waves*, vol. 45, no. 9–10, pp. 765–788, Oct. 2024, doi: 10.1007/S10762-024-01002-Y/METRICS.
- [20] M. F. A. S. Mohamed Atef Abbas, Abdelmegid Allam, Abdelhamid Gaafar, Hadia M. Elhennawy, “Compact UWB MIMO Antenna for 5G Millimeter-Wave Applications,” *Sensors*, vol. 23, no. 5, p. 2702, 2023, doi: <https://doi.org/10.3390/s23052702>.
- [21] E. A. F. A. Mostafa A. Nassar, Heba Y. M. Soliman, Rania Mohamed Abdallah, “Improving Mutual Coupling in MIMO Antennas Using Different Techniques,” *Prog. Electromagn. Res.*, vol. 133, pp. 81–95, 2023, doi: 10.2528/PIERC23033106.
- [22] T. V. and J. N. M. A. Ramos, “A Review on Mutual Coupling Reduction Techniques in mmWaves Structures and Massive MIMO Arrays,” *IEEE Access*, vol. 11, pp. 143143–143166, 2023, doi: 10.1109/ACCESS.2023.3343107.
- [23] P. N. Fletcher, M. Dean, and A. R. Nix, “Mutual coupling in multi-element array

- antennas and its influence on MIMO channel capacity,” *Electron. Lett.*, vol. 39, no. 4, pp. 342–344, Feb. 2003, doi: 10.1049/EL:20030219.
- [24] R. G. Vaughan and J. B. Andersen, “Antenna diversity in mobile communications,” *IEEE Trans. Veh. Technol.*, vol. 36, no. 4, pp. 149–172, 1987, doi: 10.1109/TVT.1987.24115.
- [25] S. Blanch, J. Romeu, and I. Corbella, “Exact representation of antenna system diversity performance from input parameter description,” *Electron. Lett.*, vol. 39, no. 9, pp. 705–707, May 2003, doi: 10.1049/EL:20030495.
- [26] S. H. K. and A. I. M. Abdullah, “Eight Element Multiple-Input Multiple-Output (MIMO) Antenna for 5G Mobile Applications,” *IEEE Access*, vol. 7, pp. 134488–134495, 2019, doi: 10.1109/ACCESS.2019.2941908.
- [27] M. Sharma, N. Choudhary, N. Kumar, S. N. Panda, and R. Kaushal, “A Slotted Hexagonal 4 $\times$ 4 MIMO Antenna with Tapered feed Designed for High Speed IoT Wireless Applications,” *Proc. IEEE Int. Conf. Signal Process. Control*, vol. 2021-October, pp. 203–208, 2021, doi: 10.1109/ISPC53510.2021.9609391.
- [28] S. H. Chae, W. Il Kawk, S. O. Park, and K. Lee, “Analysis of mutual coupling in MIMO antenna array by TARC calculation,” *Asia-Pacific Microw. Conf. Proceedings, APMC*, vol. 3, pp. 2090–2093, 2006, doi: 10.1109/APMC.2006.4429825.



Copyright © by authors and 50Sea. This work is licensed under Creative Commons Attribution 4.0 International License.